

Environmental signals in a highly resolved ice core from James Ross Island, Antarctica

Nerilie J. Abram,^{1,2} Robert Mulvaney,¹ and Carol Arrowsmith³

Received 22 April 2011; revised 8 August 2011; accepted 9 August 2011; published 22 October 2011.

[1] The accumulation, isotopic and chemical signals of an ice core from James Ross Island, Antarctica, are investigated for the interval from 1967 to 2008. Over this interval, comparison with station, satellite and reanalysis data allows for a detailed assessment of the environmental information preserved in the ice. Accumulation at James Ross Island is enhanced during years when the circumpolar westerlies are weak, allowing more precipitation events to reach the northeastern Antarctic Peninsula. The stable water isotope composition of the ice core has an interannual temperature dependence consistent with the spatial isotope-temperature gradient across Antarctica, and preserves information about both summer and winter temperature variability in the region. Sea salts in the ice core are derived from open water sources in the marginal sea ice zone to the north of James Ross Island and transported to the site by strengthened northerly and westerly winds in the winter. A strong covariance with temperature means that the sea salt record may be able to be utilized, in conjunction with the isotope signal, as an indicator of winter temperature. Marine biogenic compounds in the ice core are derived from summer productivity within the sea ice zone to the south of James Ross Island. This source region may have become significant only in recent decades, when the collapse of nearby ice shelves established new sites of open water with high summer productivity. These findings provide a foundation for interpreting the environmental signals in the James Ross Island ice core, which extends through the whole Holocene and represents the oldest ice core that has been recovered from the Antarctic Peninsula region.

Citation: Abram, N. J., R. Mulvaney, and C. Arrowsmith (2011), Environmental signals in a highly resolved ice core from James Ross Island, Antarctica, *J. Geophys. Res.*, 116, D20116, doi:10.1029/2011JD016147.

1. Introduction

[2] The ice sheets that lie over Antarctica retain chemical and physical signals that can be used to reconstruct a wide range of past environmental conditions. In central Antarctica, where the ice sheets are many kilometers thick and annual snow accumulation is low, paleoclimate reconstructions from ice cores extend back hundreds of thousands of years [EPICA community members, 2004]. In coastal areas of Antarctica, where annual accumulation is high, ice core records yield very detailed records of past climate over much shorter time periods [Thomas *et al.*, 2009; van Ommen and Morgan, 2010]. For the Antarctic Peninsula region the ice cores collected to date extend back at most a few centuries before the present-day [Aristarain *et al.*, 1990; Thompson *et al.*, 1994]. The rapid warming of the Antarctic Peninsula that has been observed over the last 50 years suggests that this region may be particularly sensitive to

climate change caused by global greenhouse gas emissions and local stratospheric ozone depletion [Vaughan *et al.*, 2003; Cook *et al.*, 2005; Turner *et al.*, 2005]. Because of this, there is a strong need to develop a longer history of the natural range of environmental variability in this region, as well as a better understanding of the connection between climate in the Antarctic Peninsula region with the rest of the Antarctic continent.

[3] This study presents an analysis of the environmental signals retained in the first ice core that has been recovered to bedrock in the Antarctic Peninsula region. The ice core was collected in January–February 2008 from James Ross Island. This island lies immediately to the east of the northern tip of the Antarctic Peninsula and is covered by a small ice cap that is approximately 50 km in diameter (Figure 1). A number of decade to century-scale ice cores have previously been collected from the James Ross Island ice cap (also known as Daling Dome) [Aristarain *et al.*, 1982, 1990; Aristarain and Delmas, 2002; Aristarain *et al.*, 2004; McConnell *et al.*, 2007]. However, the new ice core from James Ross Island now provides a record from this site that extends through the whole Holocene and into cold glacial interval ice (R. Mulvaney *et al.*, manuscript in preparation, 2011). The new James Ross Island ice core also provides a much longer

¹British Antarctic Survey, Cambridge, UK.

²Now at Research School of Earth Sciences, Australian National University, Canberra, ACT, Australia.

³NERC Isotope Geosciences Laboratory, Keyworth, UK.

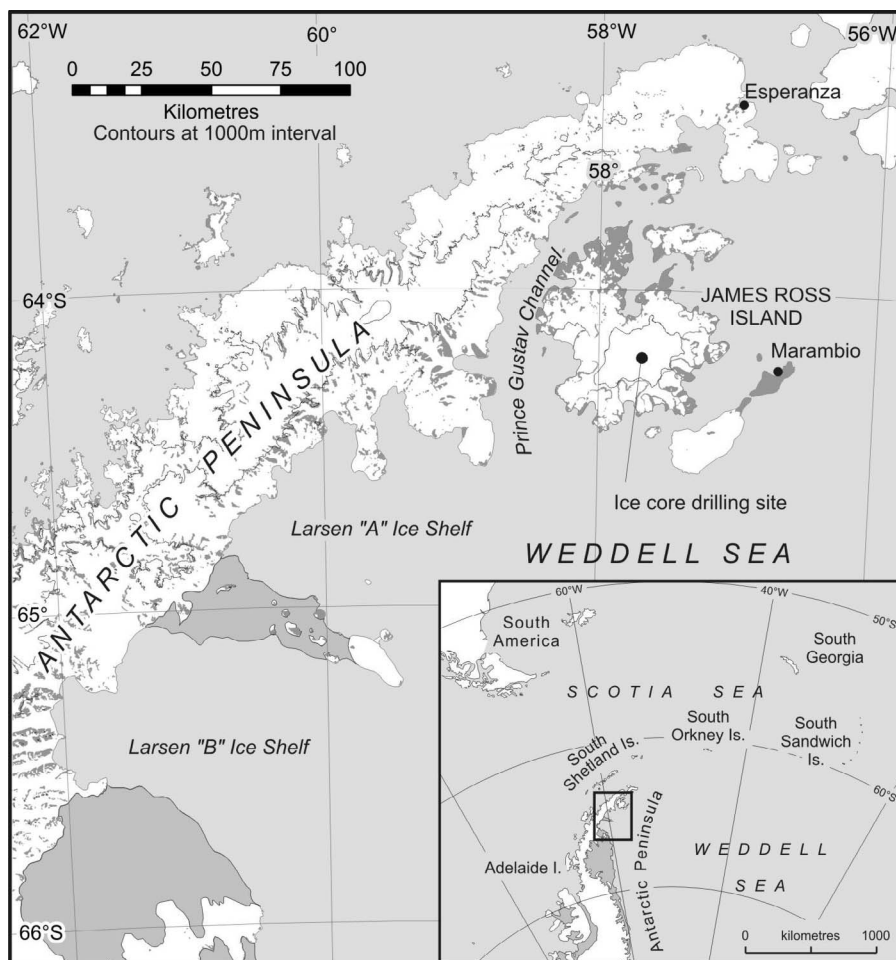


Figure 1. Regional setting of James Ross Island, which lies to the east of the northern tip of the Antarctic Peninsula. This region has undergone rapid warming in the last 50 years which has been attributed to the collapse of the nearby Prince Gustav, Larsen A and Larsen B ice shelves. Contour interval is 1000 m, and the ice core drilling site on James Ross Island lies at an elevation of 1542 m.

period of overlap with observational records of climate, compared with previous ice cores from the site that only cover the time period up until to 1990, and this allows for a more rigorous analysis than has previously been possible of the environmental signals that are being recorded in the ice at this site.

[4] Here we carry out a detailed analysis of the seasonal and interannual characteristics of the accumulation, stable water isotope and ion chemistry composition of the most recent 40 years of the James Ross Island ice core. These signals are investigated alongside instrumental, satellite and reanalysis data to develop a clear understanding of the environmental conditions and physical processes that determine the composition of the ice core. This understanding will provide a foundation for interpreting the paleoclimate reconstructions from the rest of the James Ross Island ice core, as well as giving new insights into the possible drivers of the chemical signals in ice cores from other coastal Antarctic sites.

2. Materials and Methods

2.1. Ice Core Site Details and Analysis

[5] The peak of the James Ross Island ice cap is known as Mount Haddington, and is comprised of a double peak at its

northeastern end and a broad relatively flat region stretching to the southwest. Radar studies show that on this broad shoulder the ice cap is approximately 300–400 m thick, while under the highest points of the ice cap the substrate rises to a peak and the ice thickness is reduced to only ~200 m. The James Ross Island core was drilled at $057^{\circ}41.10'W$, $64^{\circ}12.10'S$, at an altitude of 1542 m, using an electromechanical drill and a partially fluid (D60) filled hole. The core extends to bedrock at this site, which was reached at 363.9 m. The borehole thermistor profile shows a minimum temperature of $-14.38^{\circ}C$ measured at 80 m depth. This minimum borehole temperature is similar to the mean annual temperature of $-14.31^{\circ}C$ quoted in previous studies at this site [Aristarain *et al.*, 2004], although the deep location of the thermal minimum also suggests that the mean annual temperature on James Ross Island has warmed recently, consistent with abundant evidence of regional warming along the Antarctic Peninsula over at least the last 50 years [Vaughan *et al.*, 2003; Cook *et al.*, 2005; Turner *et al.*, 2005].

[6] In this study we use isotopic and chemical data derived from the upper 41 m (snow depth) of the James Ross Island ice core. Stable water isotopes were measured

Table 1. Mean Isotopic and Chemical Composition of the James Ross Island Ice Core^a

Species	Mean Annual Composition	Mean Annual Maximum ^b	Mean Annual Minimum ^b	Estimated Precision ^c
$\delta^{18}\text{O}$	−19.0‰	−18.4‰ (Jan)	−19.6‰ (Jul)	0.08‰
δD	−147‰	−143‰ (Jan)	−152‰ (Jul)	1.0‰
Na	298 $\mu\text{g g}^{-1}$	594 $\mu\text{g g}^{-1}$ (Aug)	164 $\mu\text{g g}^{-1}$ (Jan)	1.7 $\mu\text{g g}^{-1}$ (88)
Cl	470 $\mu\text{g g}^{-1}$	953 $\mu\text{g g}^{-1}$ (Aug)	244 $\mu\text{g g}^{-1}$ (Jan)	1.6 $\mu\text{g g}^{-1}$ (317)
SO_4	128 $\mu\text{g g}^{-1}$	168 $\mu\text{g g}^{-1}$ (Dec)	96 $\mu\text{g g}^{-1}$ (Jun)	0.9 $\mu\text{g g}^{-1}$ (319)
nss- SO_4	52 $\mu\text{g g}^{-1}$	108 $\mu\text{g g}^{-1}$ (Jan)	−2.3 $\mu\text{g g}^{-1}$ (Aug)	
MSA	17 $\mu\text{g g}^{-1}$	25 $\mu\text{g g}^{-1}$ (Jan)	8.9 $\mu\text{g g}^{-1}$ (Jul)	0.4 $\mu\text{g g}^{-1}$ (305)

^aMean annual, maximum and minimum climatology (and mean month of occurrence) for the 1967–2008 portion of the core presented here. The calculation of nss- SO_4 data used Na as the sea salt reference species.

^bMonth of maximum and minimum is given in parentheses.

^cNumber of duplicates is given in parentheses.

on 11 cm resolution samples at the NERC Isotope Geosciences Laboratory. The samples were equilibrated with CO_2 using an Isoprep 18 device for oxygen isotope analysis with mass spectrometry preformed on a VG SIRA 10. For hydrogen isotope analysis, an online Cr reduction method was used with a EuroPyrOH-3110 system coupled to a Micromass Isoprime mass spectrometer. Analytical precision is typically 0.08‰ for $\delta^{18}\text{O}$ and 1.0‰ for δD . For part of the record, 5 cm and 2.5 cm stable water isotope samples were also analyzed at the British Antarctic Survey on a Los Gatos Research DLT-100 cavity ringdown laser spectroscopy instrument with a precision of typically 1.0‰ for δD . The laser spectroscopy data showed excellent agreement with δD measurements made by mass spectrometry but did not yield any additional detail over the 11 cm resolution isotope results, presumably due to a high rate of isotopic diffusion at this relatively warm site that smoothes much of the high-frequency detail in the isotopic profile [Cuffey and Steig, 1998; Johnsen *et al.*, 2000]. Accordingly, in this paper we only use the stable water isotope data obtained by the mass spectrometry method.

[7] Samples for ion chromatography analysis were cut at 5 cm resolution before being melted and analyzed in a class 100 clean laboratory at the British Antarctic Survey [Littot *et al.*, 2002]. Anion measurements were carried out using a Dionex ICS-2500 ion chromatograph with a 2mm AG17-AS17 column set and 2mm ASRS suppressor using a KOH eluent generator cartridge running on a gradient concentration program from 1 mM to 40 mM. Cation measurements were performed using a Dionex ICS-2000 ion chromatograph with a 3mm CG12-CS12 column set and 2 mm CSRS suppressor using a methanesulphonic acid eluent generator cartridge operating isocratically at 20 mM concentration. Table 1 gives the mean concentration of each species in the James Ross Island ice, as well as the estimated precision calculated from the mean concentration difference of duplicate measurements of the James Ross Island ice samples.

[8] The most recent 40 years of the James Ross Island ice core presented in this paper were dated using the annual cycles in non-sea salt sulphate (nss- SO_4 ; calculated using Na as the sea salt reference), which provided the clearest cyclicity of all of the chemical components (Figure 2). A five point running mean was used to assign the depth of the

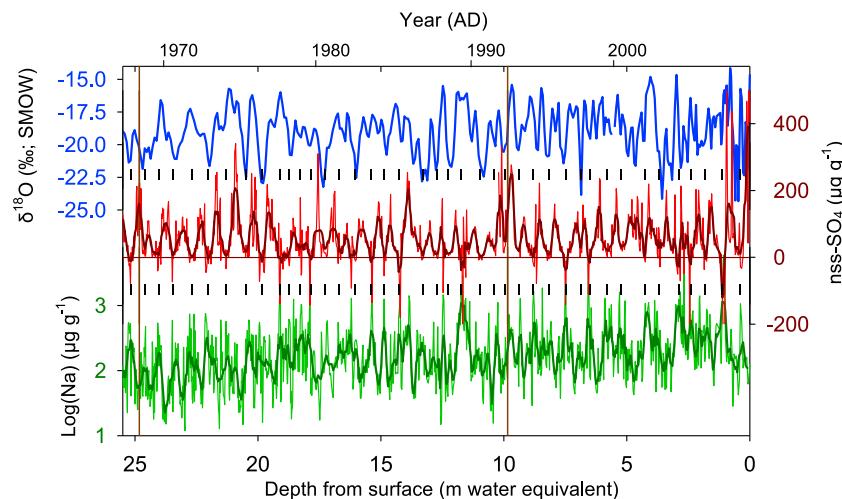


Figure 2. Example of the chemical signals in the James Ross Island ice core. The 11 cm resolution $\delta^{18}\text{O}$ (blue) and 5 cm resolution nss- SO_4 (red line) and Na (green line; shown as $\log(\text{Na})$) records are displayed on a water equivalent depth scale. Thick red and green lines are a 5-point running mean. Black dashes show the location of the assigned annual markers, based primarily on the minimum in the 5-point running mean of nss- SO_4 . Brown vertical lines indicate the position of a visible tephra layer attributed to the December 1967 eruption of the Deception Island volcano, and the start of a broad elevated nss- SO_4 peak that occurred following the 1991 eruption of Pinatubo.

annual minimum in nss-SO₄, with cycles of oxygen isotope ratios and sodium providing additional guidance on determining the annual marker depths. The annual marker age scale at the bottom of this 40 year section is constrained by a visible tephra layer with associated elevated fluoride concentrations at 40.035 m snow depth in the core. These are attributed to the December 1967 eruption of the Deception Island volcano that is documented to have produced a layer of ash in the James Ross Island area [Delmas *et al.*, 1985]. A broad interval of elevated nss-SO₄ concentrations beginning at 18.05 m snow depth may also be attributed to the 1991 eruption of Pinatubo in the Philippines, while comparison of our chemical profiles with the surface age control markers provided by the succession of previous ice cores from James Ross Island [Aristarain *et al.*, 2004] also confirms that the annual layer chronology in this upper section is robust.

[9] The 5 cm resolution sampling equates to an average of 20 samples per year over this portion of the James Ross Island record. To enable an investigation of the chemical components alongside observational records, each of the unsmoothed chemical signals was linearly interpolated to produce monthly resolution records. Assigning the annual chronology markers (based on the minimum in the 5-point smoothed nss-SO₄ signal) to the month of July results in a mean seasonal cycle of the stable water isotope signals which has a maximum in January and minimum in July (Table 1), consistent with the climatology for the warmest and coldest months in this region. Within the annual cycle, we estimate that errors in the interpolated age scale are likely on the order of ± 2 months.

2.2. Observational Data Sets

[10] A range of data sets are used for the analysis of the environmental signals preserved in the James Ross Island ice core. First we use the monthly observations of temperature and mean sea level pressure (MSLP) at Esperanza Station, which is located on the northern tip of the Antarctic Peninsula approximately 96 km to the north of the drilling site on James Ross Island and sits at an elevation of 13 m. Meteorological observations from Esperanza station began in 1945 and constitute the most continuous and reliable instrumental record available for the northern Antarctic Peninsula. Results based on the Esperanza observations are also verified by repeating the analysis with data from Marambio station, which is situated on Seymour Island 52 km to the east of the drilling site on James Ross Island. Marambio station has an elevation of 198 m and observational data are available since 1971, but are sporadic from 1992 to 1995.

[11] We also use the reanalysis products from the European Centre for Medium range Weather Forecasts (ECMWF) to investigate the spatial relationships between chemical signals in the James Ross Island core and the climate fields available for MSLP, zonal and meridional wind stress, surface air temperature and precipitation. In these reanalysis products southerly and westerly wind anomalies are denoted by positive wind stress values. We primarily use the new ERA-Interim reanalysis, which is available from 1989 to present [Berrisford *et al.*, 2009]. ERA-Interim has a higher spatial ($0.7^\circ \times 0.7^\circ$) and height resolution and improved model physics and characterization of the hydrological cycle compared with the earlier ERA-40 reanalysis. A recent

assessment for the Amundsen Sea region of Antarctica has shown ERA-Interim to be the most reliable, at least for this region of Antarctica, of all of the reanalysis products currently available (T. J. Bracegirdle, Climatology and recent increase of westerly winds over the Amundsen Sea derived from six re-analyses, submitted to *International Journal of Climatology*, 2011). We also verify our findings using the older, lower-resolution ($2.5^\circ \times 2.5^\circ$) ERA-40 reanalysis data which provides reanalysis fields from 1957 until 2002 [Uppala *et al.*, 2005]. The ERA-40 data is used since 1979, when the assimilation of satellite data is believed to make the reanalysis reasonably reliable for Antarctica [Marshall, 2003; Thomas and Bracegirdle, 2009]. The ERA-40 model is known to have some limitations in the Antarctic Peninsula region, including James Ross Island, as it is unable to sufficiently resolve the steep mountainous barrier of the Antarctic Peninsula [Miles *et al.*, 2008].

[12] Finally, we also use satellite data sets to examine the relationship of sea salt and marine biogenic signals in the James Ross Island ice core with sea ice and productivity around Antarctica. Gridded sea ice concentration data are available for Antarctica from 1978 to present-day. We use data that is processed using the NASA team algorithm [Cavalieri and Parkinson, 2008] and archived at the National Snow and Ice Data Centre [Cavalieri *et al.*, 2008]. We also use SeaWiFS (Sea-viewing Wide Field-of-View Sensor) satellite data for chlorophyll-a concentration as a measure of ocean primary productivity [McClain *et al.*, 2004; Acker and Leptoukh, 2007]. SeaWiFS chlorophyll-a data are available from 1997 to 2010, although in the Antarctic the record is discontinuous through the Austral winter period.

3. Results and Discussion

[13] To understand the seasonal characteristics of climate in the James Ross Island region we first used the Esperanza station observations as well as the ERA-Interim reanalysis data bi-linearly interpolated to the drilling site to construct composite seasonal cycles for the various climatic parameters in this area. To test the regional significance of interannual variability, spatial correlations were also performed for the Esperanza record against the ERA-Interim reanalysis fields.

[14] The seasonal cycle in MSLP shows highest pressures in June and lowest pressures in October (Figure 3a). There is an excellent agreement seen in the pattern of the seasonal cycle as well as the absolute values between the Esperanza record and the interpolated MSLP at the James Ross Island drill site from the ERA-Interim reanalysis. The corresponding seasonal cycle in ERA-Interim zonal wind stress shows that at James Ross Island the climatological winds are always westerly, and are weakest in January and strongest in September. The seasonal cycle in meridional winds shows a slight tendency for weak northerly winds from August to February, and southerly winds from March to July that peak in June. However, the 1σ spread in the seasonal composite spans across southerly and northerly meridional winds for all months. On an interannual time scale, correlation of Jan–Dec annual averages of the Esperanza MSLP record with the annually averaged ERA-Interim MSLP field shows that interannual variability in MSLP at Esperanza is

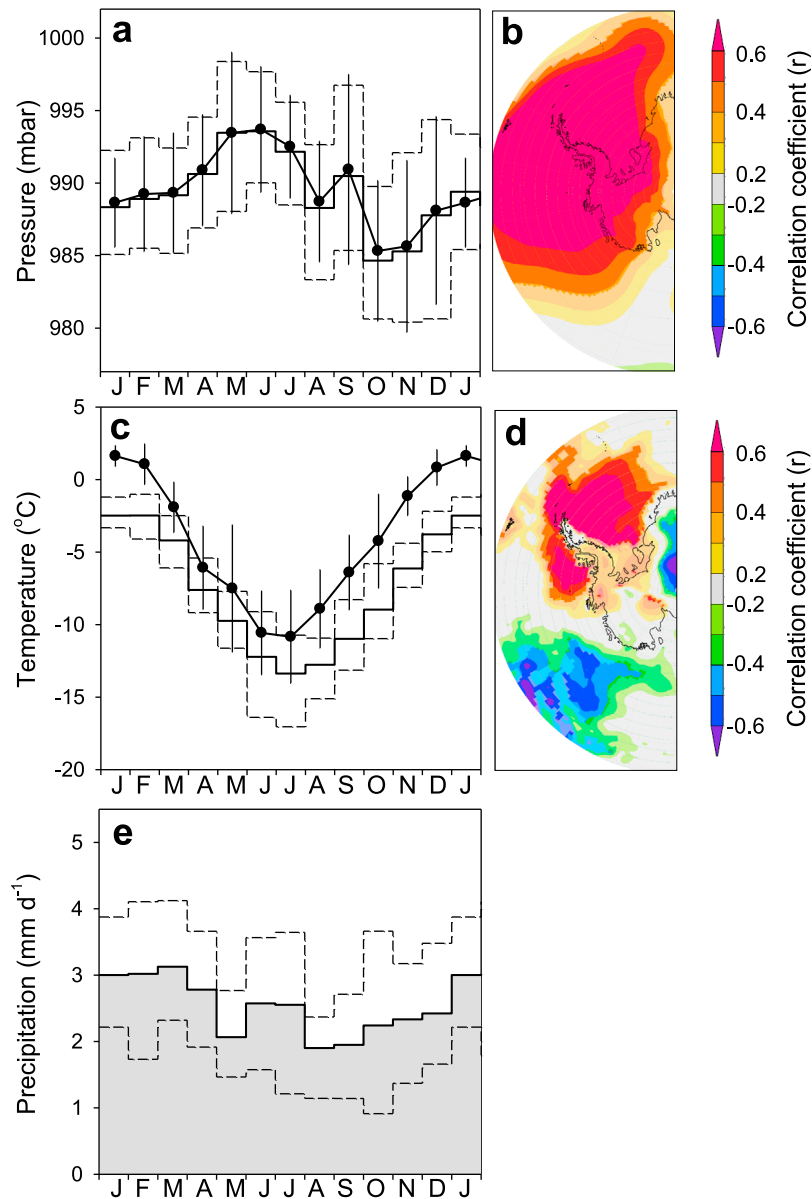


Figure 3. (a) The mean annual cycle (1989–2008) of sea level pressure measured at Esperanza station (circles) and given by ERA-Interim reanalysis bi-linearly interpolated to the James Ross Island drill site (solid horizontal line plot). The 1σ range on the mean monthly values for the Esperanza and ERA-Interim data are shown by error bars and dashed lines, respectively. (b) Spatial correlation of annual average (Jan–Dec) observations of sea level pressure at Esperanza with the ERA-Interim sea level pressure reanalysis fields. Correlations that fall below 90% confidence are masked. (c and d) Details as for Figures 3a and 3b, using surface air temperature observations from Esperanza and the ERA-Interim reanalysis. (e) Mean monthly precipitation (and 1σ range) at James Ross Island from the ERA-Interim reanalysis.

representative of MSLP spanning across a broad geographical region (Figure 3b). Together, the seasonal and interannual correspondence in MSLP gives us confidence that interannual variability in both the Esperanza and ERA-Interim MSLP data sets is reliable and representative of conditions on James Ross Island.

[15] The mean seasonal cycle in temperature at Esperanza station shows a maximum in January of 1.6°C and a minimum in July of -10.8°C (Figure 3c). Marambio station shows an equivalent annual cycle but is ~ 2 – 3 degrees cooler than Esperanza. The ERA-Interim reanalysis temperature

for the James Ross Island site, shows a similar timing and magnitude of the seasonal temperature cycle, but the absolute values are ~ 3 – 4 degrees cooler than those recorded at Esperanza station. The spatial correlation of interannual temperature variability at Esperanza with ERA-Interim surface air temperature shows significant correlations over the Weddell Sea and the Bellingshausen Sea. However, correlations are below the 90% confidence threshold for the narrow strip of grid squares that encompass the Antarctic Peninsula (Figure 3d). The same absence of significant interannual correlations along the Antarctic Peninsula is

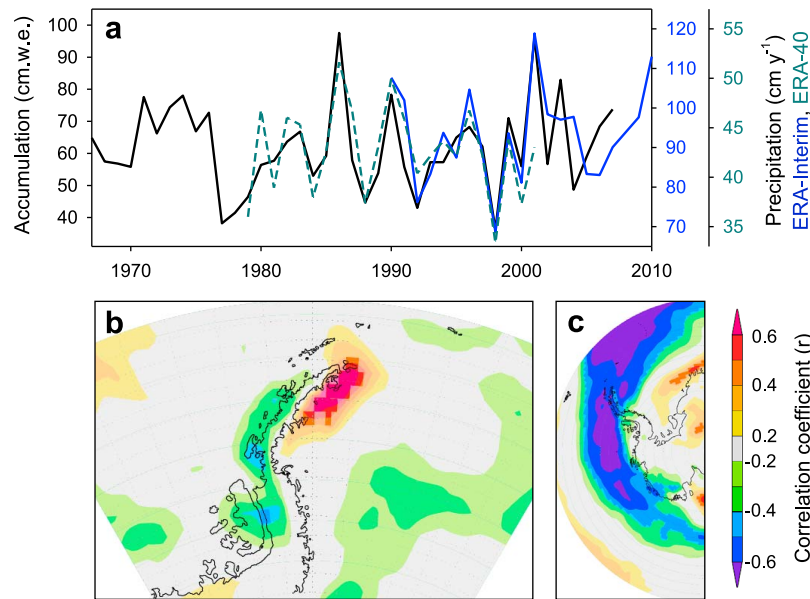


Figure 4. (a) Mean annual (Jul–Jun) accumulation in the James Ross Island core (black curve) compared with ERA-Interim (blue solid) and ERA-40 (green dashed) precipitation bi-linearly interpolated to the James Ross Island drill site. Note the offset in the absolute scales. Spatial correlation of accumulation at James Ross Island with July–June averages of (b) ERA-Interim precipitation and (c) ERA-Interim zonal wind stress (1989–2008). Years of high accumulation at the James Ross Island site are a localized feature of the northeastern side of the Antarctic Peninsula and correspond with years when the circumpolar westerly winds are weakened. Correlations that fall below 90% confidence are masked.

observed using the Marambio observational temperature record and using the ERA-40 reanalysis. This may represent a deficiency in the ability of the ERA-Interim and ERA-40 reanalysis to translate patterns of MSLP into reliable records of interannual temperature variability along the high topography of the Antarctic Peninsula. Alternately, it could indicate that interannual temperature variability observed at coastal sites around the Antarctic Peninsula is not representative of the interannual temperature variability at higher altitude sites along the Antarctic Peninsula. The true cause of this discrepancy is difficult to assess in the absence of continuous, multiyear weather station observations from non-coastal sites on the Antarctic Peninsula. Accordingly, in this paper we assess the temperature influence on the chemical composition of the James Ross Island ice core using both ERA reanalysis and station observational data.

[16] Precipitation in the ERA-Interim reanalysis for James Ross Island ranges from a minimum of $2.6 \pm 1.0 \text{ mm d}^{-1}$ in August to a maximum of $3.9 \pm 1.3 \text{ mm d}^{-1}$ in February, suggesting that snow accumulation at the site should be high and reasonably constant throughout the year (Figure 3e). Following the concept of *Sime et al.* [2009], we investigated the likelihood of accumulation variability biasing the environmental signal preserved at this site by calculating a precipitation-weighted temperature time series. Using daily temperature and precipitation data in the ERA-Interim reanalysis, and a geometric mean regression method to minimize the uncertainty in both the temperature (T) and precipitation-weighted temperature (TP) dimensions [Smith, 2009], we calculate a slope of $1.18 \pm 0.23(\text{SE})$ for Jul–Jun annual averages at the James Ross Island site. Using a least squares regression method that only minimizes the uncer-

tainty in the TP dimension yields a slope of 0.66 ± 0.23 . Similar (within error) results are obtained using the ERA-40 reanalysis. Thus, for the interval of time covered by the ERA reanalysis products there isn't a clear indication that precipitation covariance should either enhance or diminish the interannual temperature variability preserved in the ice core from James Ross Island.

3.1. Accumulation

[17] For the upper 40 years of the James Ross Island ice core the mean accumulation rate is $0.62 \pm 0.14 \text{ m}$ of water equivalent per year, based on the annual chronology derived from the winter nss-SO₄ markers. This is considerably higher than the previously reported annual average accumulation rate of 0.40 m for the James Ross Island ice cap [Aristarain and Delmas, 2002; Aristarain et al., 2004]. However, this value may be a mean accumulation calculated over a longer time period than discussed here as the data presented for previous ice cores from James Ross Island suggest that accumulation on the ice cap was $\sim 0.59 \text{ m}$ per year for the overlapping interval from 1967 to 1990 [e.g., see Aristarain et al., 2004, Figure 2].

[18] Interannual variability of July–June accumulation at the James Ross Island site is strongly correlated with precipitation variability in the ERA-Interim ($r = 0.72$, $p = 0.0008$) and ERA-40 ($r = 0.65$, $p = 0.0007$) reanalysis (Figure 4a). We do note that snow accumulation at the site will be influenced not only by precipitation, but also by snow loss through ablation and redistribution by wind drifting. However, the strong correlations with precipitation in the ERA reanalysis suggest that precipitation is the dominant source of accumulation variability at this site. In

terms of absolute values, for ERA-Interim the amount of precipitation is slightly higher than the accumulation preserved in the James Ross Island core, perhaps owing to the unaccounted loss of snow through ablation. For ERA-40, the amount and range of precipitation is markedly lower than that preserved in the accumulation record from the James Ross Island site. Problems with the ERA-40 precipitation at James Ross Island have been discussed previously and attributed to the low resolution of ERA-40 yielding a poor representation of the topography here [Miles *et al.*, 2008]. However, our findings suggest that at least in terms of the pattern of interannual variability, precipitation in both ERA-40 and ERA-Interim is representative of accumulation variability at James Ross Island.

[19] Spatial correlation with precipitation in the ERA-Interim reanalysis field shows that high accumulation at the James Ross Island site is associated with high precipitation in a geographically limited region along the northeastern side of the Antarctic Peninsula (Figure 4b). At the same time, reduced precipitation occurs along the western and southern regions of the Antarctic Peninsula. This precipitation pattern along the Antarctic Peninsula is associated with a reduction in the strength of the westerly winds in the ERA-Interim reanalysis (Figure 4c). This suggests that when the circumpolar westerlies are weak the orographic rain shadow effect of the Antarctic Peninsula may be reduced, resulting in less precipitation on the western side of the Peninsula and allowing more storm events to deliver precipitation to the northeastern region of the Antarctic Peninsula [Miles *et al.*, 2008]. The opposing northeast-southwest patterns of accumulation variability across the Antarctic Peninsula suggests that comparing the accumulation record of the James Ross Island ice core with similar accumulation records from sites like Dyer Plateau and Gomez on the southwestern Antarctic Peninsula [Thompson *et al.*, 1994; Thomas *et al.*, 2008] has the potential to yield important insights into the spatial pattern of changes in accumulation on the Antarctic Peninsula and their connection to climate features such as the Southern Annual Mode (SAM) [Marshall, 2003; Miles *et al.*, 2008].

3.2. Stable Water Isotope Ratios

[20] Stable water isotopes ($\delta^{18}\text{O}$ and δD) in ice are the most widely used proxy in ice core studies. The ratio of heavy to light water molecules in precipitation is influenced by the source temperature and isotopic composition where evaporation occurs, the distance over which the evaporate travels and the site temperature when the precipitation falls [Masson-Delmotte *et al.*, 2008]. For paleoclimate interpretations it is often assumed that changes in source temperature/location are negligible and that changes in the stable water isotope composition of ice primarily reflect changes in temperature at the ice core site. The use of isotope-enabled climate models can help to reduce or eliminate these assumptions, but such models do not have sufficiently high resolution at present to be utilized in the interpretation of ice core records from the Antarctic Peninsula region [Sime *et al.*, 2008; Stenni *et al.*, 2010]. The lack of suitable temporal calibration data at many sites also means that the modern day spatial relationship between site temperature and stable water isotope composition in Antarctica is frequently used in ice core paleoclimate reconstructions to

estimate the temperature change associated with stable water isotope changes [Jouzel *et al.*, 2003; Masson-Delmotte *et al.*, 2008].

[21] The $\delta^{18}\text{O}$ and δD composition of the James Ross Island ice core are highly correlated ($r = 0.99$, $n = 470$) and covary with a ratio of 8.02 ± 0.04 that matches the slope of the meteoric water line. The mean annual cycle in $\delta^{18}\text{O}$ and δD in the James Ross Island ice core agrees closely with the shape of the seasonal temperature cycle in this region; the age scale linearly interpolated between the winter nss-SO_4 minimum results in mean seasonal isotopic minimum and maximum that fall in July and January, respectively (Table 1), both matching the seasonal timing of minimum and maximum temperatures in this region. This supports the indications from ERA-Interim reanalysis for reasonably constant precipitation throughout the year at James Ross Island that does not appreciably bias the preserved isotopic record at this site toward a particular season. The magnitude of the seasonal cycle of stable water isotopes is small compared to the expected magnitude of the Antarctic isotope-temperature dependence [Masson-Delmotte *et al.*, 2008]. This most likely reflects the noted smoothing of the high frequency (cm scale) isotope signal by diffusion and needs to be further assessed for this site using isotope-enabled transport and diffusion modeling. The high accumulation at James Ross Island means that isotopic diffusion processes should not alter the interannual isotopic record.

[22] On an interannual time scale, the mean annual isotopic content of James Ross Island ice correlates significantly with the temperature record from Esperanza and Marambio stations, as well as the temperature records from the ERA-Interim and ERA-40 reanalysis for the James Ross Island site (Table 2 and Figure 5). The relationships are also significant when calculated using just the summer (Oct–Mar) or winter (Apr–Sep) halves of the isotope and temperature records, indicating that the isotopic composition of the James Ross Island ice core preserves information about both summer and winter temperature variability. Using the precipitation-weighted temperature record [Sime *et al.*, 2009] calculated from the ERA-Interim data for James Ross Island does not increase the correlation with isotopes in the James Ross Island core, further indicating that the interannual temperature information preserved in the stable water isotopes at this site is not significantly biased by precipitation variability. Correlations of the stable water isotope record with reanalysis zonal and meridional winds suggest that, on an interannual time scale, westerly and to a lesser extent northerly wind anomalies at James Ross Island are associated with warmer temperatures at the ice core site.

[23] Spatial correlation maps for ERA-Interim reanalysis fields (Figure 6) show that different climatological features are associated with summer and winter isotopic variability at James Ross Island. For summer (Oct–Mar) averages, warmer isotopic temperatures are associated with a broad low pressure anomaly over the Antarctic continent and a band of high pressure anomalies in the mid latitude regions, along with westerly wind anomalies encircling Antarctica (Figures 6a–6d). This is characteristic of the SAM [Marshall, 2003], and indeed the summer isotopic composition of the James Ross Island ice core does have a significant correlation with the SAM index ($\delta^{18}\text{O}$, $r = 0.38$, $p = 0.017$; δD , $r = 0.36$, $p = 0.025$). For winter (Apr–Sep)

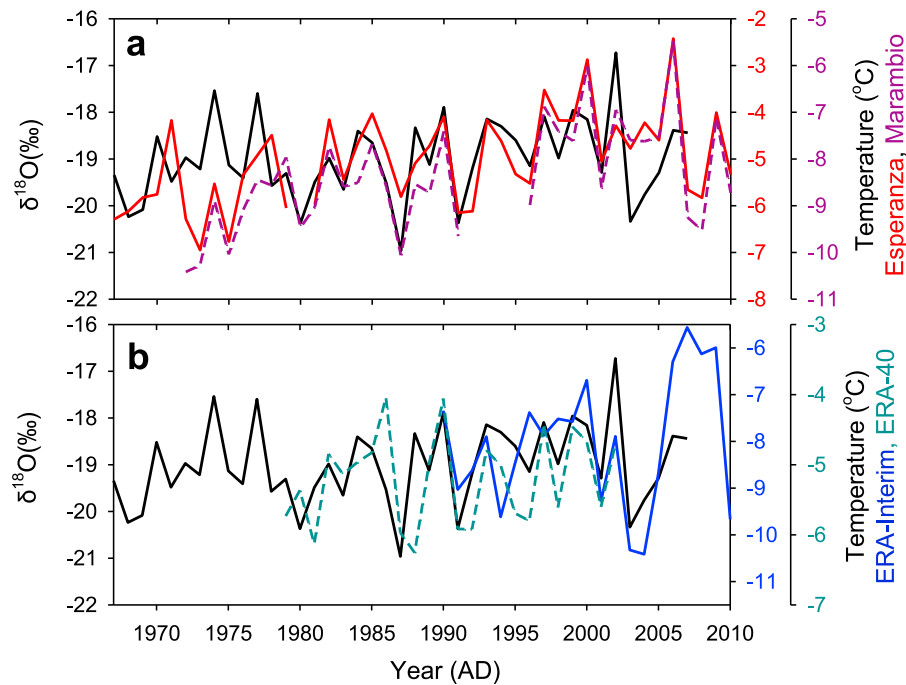


Figure 5. Time series of Jul–Jun annual averages of $\delta^{18}\text{O}$ in the James Ross Island ice core (black solid) with (a) temperature at Esperanza (red solid) and Marambio (purple dashed) stations and (b) from ERA-Interim (blue solid) and ERA-40 (cyan dashed) temperature bi-linearly interpolated to the James Ross Island drill site. Note that the observational and reanalysis temperature scales are shown for different absolute temperatures but with the same range of temperature change, except for ERA-40 which has a lower magnitude of interannual temperature variability at this site.

averages, warmer isotopic temperatures at James Ross Island are correlated with a wave train pattern in MSLP with nodes of high pressure in the southeastern Pacific Ocean and south Atlantic Ocean separating a low pressure feature in the Amundsen Sea. This pressure pattern is a noted feature of the Amundsen Sea Low, and its connection to climate variability of the Pacific Ocean through the Pacific – South America transpolar index [Kreutz *et al.*, 2000]. At the James Ross Island site, warm winter anomalies are strongly associated with northerly wind anomalies across Drake Passage and the Antarctic Peninsula and westerly wind anomalies across the northern Weddell Sea related to flow between the Amundsen Sea low pressure and South Atlantic high pressure features (Figures 6e–6h).

[24] We examined the interannual isotope–temperature dependence at James Ross Island by using a geometric mean regression of July–June averages of Esperanza temperature with $\delta^{18}\text{O}$ and δD . For $\delta^{18}\text{O}$, a sensitivity of $0.86 \pm 0.13(\text{SE})$ ‰ °C^{−1} is found. Repeating this calibration using ERA-Interim temperature yields a similar relationship of 0.70 ± 0.14 ‰ °C^{−1}. These interannual $\delta^{18}\text{O}$ –T slopes for James Ross Island are consistent with the well-established spatial $\delta^{18}\text{O}$ –T relationship for Antarctica of 0.80 ± 0.01 ‰ °C^{−1} [Masson-Delmotte *et al.*, 2008], which is calculated over a much larger range of temperatures and is subject to much smaller uncertainties in both dimensions. Using ERA-40 temperature gives a higher $\delta^{18}\text{O}$ –T dependence of 1.43 ± 0.26 ‰ °C^{−1}, and it seems likely that while ERA-40 tem-

Table 2. Correlation Statistics for the Relationship Between Isotopic Composition of the James Ross Island Core and Instrumental and Reanalysis Records^a

	$\delta^{18}\text{O}$			δD		
	r	p	n	r	p	n
Esperanza temperature	0.42	0.0083	38	0.46	0.0046	36
Marambio temperature	0.46	0.0089	32	0.50	0.0049	36
ERA-40 surface air temperature	0.51	0.013	23	0.53	0.0089	23
ERA-Interim surface air temperature	0.56	0.015	18	0.63	0.0085	16
ERA-Interim zonal wind stress	0.53	0.024	18	0.54	0.032	16
ERA-Interim meridional wind stress	−0.37	0.13	18	−0.44	0.085	16
ERA-Interim precipitation	−0.12	0.64	18	−0.11	0.69	16
Esperanza temperature (Oct–Mar)	0.45	0.0045	38	0.48	0.0030	36
Esperanza temperature (Apr–Sep)	0.54	0.0003	40	0.52	0.0008	38

^aReanalysis time series used for the correlations were bi-linearly interpolated to the James Ross Island drill site. All correlations are for July–June annual averages, except for the Esperanza correlations for summer (Oct–Mar) and winter (Apr–Sep) which are shown for comparison.

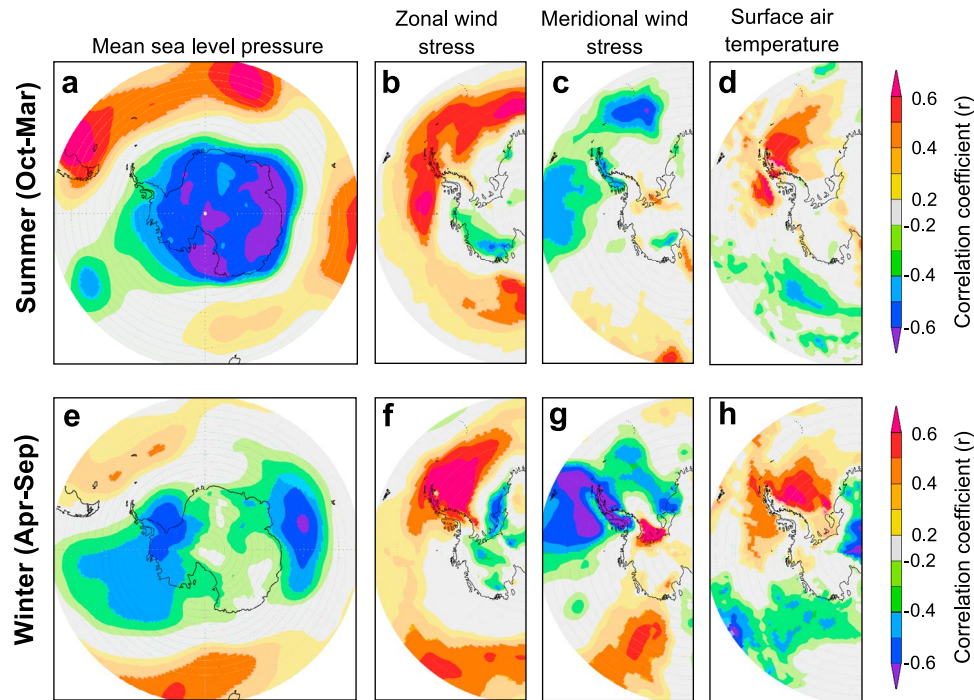


Figure 6. Correlation of summer (Oct–Mar) averages of $\delta^{18}\text{O}$ in the James Ross Island core with (a) mean sea level pressure, (b) zonal wind stress, (c) meridional wind stress and (d) surface air temperature in the ERA-Interim reanalysis (1989–2008). (e–h) As for Figures 6a–6d but using winter (Apr–Sep) averages. Correlations that fall below 90% confidence are masked.

perature captures the interannual variability of temperature at the James Ross Island site it underestimates the magnitude of this temperature variability (Figure 5b; similar also to the observed difference in scale between ice core accumulation and ERA-40 precipitation at this site, section 3.1). For δD , a temperature dependence of $6.9 \pm 1.0 \text{ ‰ } ^\circ\text{C}^{-1}$ is found with Esperanza temperature, and a similar dependence of $6.4 \pm 1.3 \text{ ‰ } ^\circ\text{C}^{-1}$ is derived using ERA-Interim temperature at James Ross Island. These relationships are again consistent with the spatial δD -T slope for Antarctica of $6.34 \pm 0.09 \text{ ‰ } ^\circ\text{C}^{-1}$ [Masson-Delmotte *et al.*, 2008].

[25] If a least squares regression method is used, a lower temporal $\delta^{18}\text{O}$ -T slope of $0.37 \pm 0.13 \text{ ‰ } ^\circ\text{C}^{-1}$ is obtained with Esperanza temperature, or $0.39 \pm 0.14 \text{ ‰ } ^\circ\text{C}^{-1}$ using ERA-Interim temperature. For δD , reduced temperature dependencies of $3.2 \pm 1.0 \text{ ‰ } ^\circ\text{C}^{-1}$ and $3.8 \pm 1.3 \text{ ‰ } ^\circ\text{C}^{-1}$ are found for Esperanza and ERA-Interim temperature, respectively, using the least squares regression method. The lower slopes occur because the least squares method assumes that there is no uncertainty in the x (temperature) dimension and fits a line that only reduces error in the y (isotope) dimension. This results in an underestimation of the slope if there is also uncertainty in the x-dimension [Solow and Huppert, 2004; Smith, 2009]. Using a least squares regression method, a similarly low δD -T slope of $4.5 \text{ ‰ } ^\circ\text{C}^{-1}$ (equivalent to a $\delta^{18}\text{O}$ -T slope of $0.56 \text{ ‰ } ^\circ\text{C}^{-1}$) was derived for an earlier James Ross Island ice core [Aristarain *et al.*, 1990]. The difference in results obtained using the two different regression methods highlight the importance of using the most appropriate technique for a particular data set.

[26] In our situation, the temporal isotope-temperature calibrations based on the geometric mean regression method are likely more appropriate as there is uncertainty in knowing the exact temperature to which the measured isotope values correspond. These uncertainties arise from errors in the intra-annual dating of the ice core as well as the lack of a directly measured temperature record for the drill site. The geometric mean regression method is also more appropriate for reconstructing past temperature, when the isotope record becomes the known (x dimension) parameter that is used to deduce past temperatures. This is because the geometric mean relationship minimizes error in both dimensions so the inverted slope yields an equivalent relationship. Using isotope-temperature calibrations based on a least squares regression, where the inverted relationship is often not equivalent, has the potential to overestimate reconstructions of past temperature changes [Solow and Huppert, 2004; Smith, 2009]. For these reasons, though we report calibration values for the James Ross Island isotope signal using both regression methods, we recommend the use of the geometric mean regression results for paleo-temperature reconstructions from this core.

3.3. Sea Salt Concentrations

[27] Sea salt species are present in high concentrations in the James Ross Island ice core. The interpretation of sea salts as an environmental proxy is still the subject of some debate, and it is likely that different processes dominate the sea salt signal at different sites. Initially believed to represent an open water source, the sea salt content of ice cores has often been interpreted as a proxy for storminess and wind-driven transport over the open ocean [Petit *et al.*,

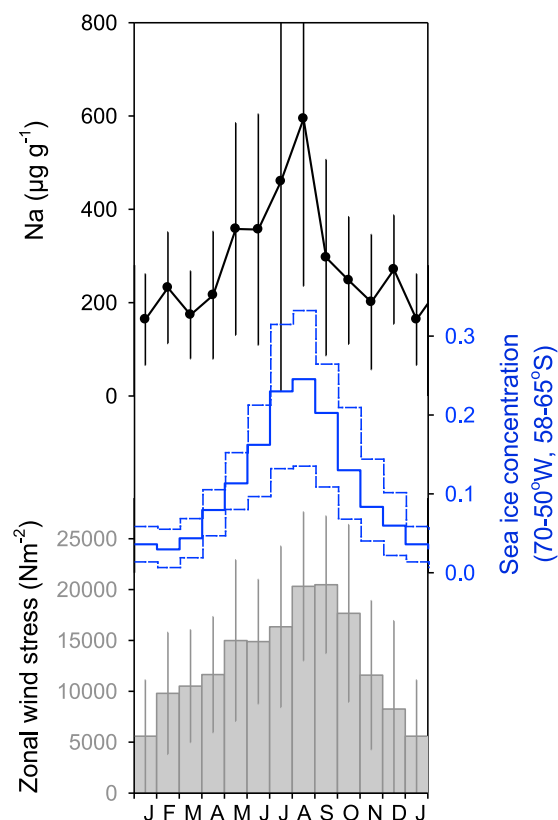


Figure 7. The composite annual cycle of Na (black circles) is shown alongside the annual cycles of sea ice concentration in the region 70–50°W, 58–65°S (blue solid line) and ERA-Interim zonal wind stress at James Ross Island (gray bars). Error bars/dashed vertical line plots give the 1σ range on the composite monthly means.

1999]. More recently, based on the observed winter maximum in sea salt and the occurrence of negative nss-SO₄ values [Wolff *et al.*, 2003; Rankin *et al.*, 2004], it has been suggested that brine on the surface of sea ice could instead represent an important source of sea salt in Antarctic ice. Using this process, changes in ice core sea salt concentrations have been interpreted as a proxy for the amount of sea ice around Antarctica [Wolff *et al.*, 2006; Fischer *et al.*, 2007; Rothlisberger *et al.*, 2010].

[28] Previous work on an ice core from James Ross Island suggested that sea salt species tended to be summer dominated at this site, coming from open water sources [Aristarain *et al.*, 2004]. The detailed analysis performed here on Sodium (Na) and Chloride (Cl) concentrations in the James Ross Island ice core instead shows that sea salt is present in high concentrations throughout the year but with a clear winter maximum that peaks around August (Figure 7 and Table 1). The correlation results presented below use Na as the representative sea salt species, however the same results (with similar levels of significance) are found by instead using the Cl record from the James Ross Island ice core. Following other studies [e.g., Rothlisberger *et al.*, 2010], our correlation analysis uses the log value of Na due to the nonlinear nature of seasonal changes in sea salt concentration.

[29] On interannual time scales, increased annual (Jan–Dec) average Na concentration in the ice core is associated with westerly and northerly wind anomalies at the James Ross Island site. Most of the significant correlation with annual Na is derived from the wind anomalies that occur in the winter (Apr–Sep) half of the year. This coincides with the seasonal timing of highest sea salt concentrations in the core and strongest winds at the James Ross Island site, and indicates a strong wind-driven influence on the amount of sea salt deposited at James Ross Island. The spatial correlation pattern of Na with the ERA-Interim reanalysis fields (Figures 8a–8d) shows the same pattern of MSLP, wind and temperature anomalies (but with higher significance) as was seen for the winter isotope record from James Ross Island (Figure 6). Thus the significant correlation of sea salt with westerly and northerly wind anomalies at the James Ross Island site appears to be representative of winter circulation patterns between the Amundsen Sea Low and high pressure anomalies in the south Atlantic Ocean.

[30] Spatial correlation of Na with the NASA satellite record of sea ice concentration (Figure 8e) shows that a negative correlation exists between the concentration of sea ice near James Ross Island and the amount of sea salt deposited on the James Ross Island ice cap. The correlation of increased annual average sea salt in the ice core with decreased sea ice concentration again predominantly reflects winter (Apr–Sep) sea ice conditions. The region of significant correlations is located in the marginal sea ice zone immediately to the north of James Ross Island and extends eastward across the northern Weddell Sea and westward along the Bellingshausen Sea margin of the Antarctic Peninsula. Winter sea ice coverage across the region spanning 70–50°W, 58–65°S has a correlation value of $r = -0.64$ ($p = 0.0002$, $n = 29$) with annual average Na in the James Ross Island core (Figure 8f). This inverse relationship between Na and sea ice in the adjacent regions indicates that at the coastal James Ross Island site open water sources are the primary source of sea salt.

[31] Together these findings show that sea salt at James Ross Island primarily comes from open water sources and is transported by northwesterly winds. The reliance on wind driven transport can account for the apparent ambiguity in the seasonal relationship between sea salt and sea ice [Wolff *et al.*, 2003], whereby the seasonal maximum of sea salt coincides with the winter maximum in sea ice coverage (Figure 7). During the summer minimum in sea ice when local open water is at its maximum, the wind strength is likely too weak to transport large amounts of sea salt to James Ross Island. Instead, sea salts in the James Ross Island core are highest during the interval of sea ice formation to the sea ice maximum, representing the confluence of intensifying westerly winds traveling over areas that are still free of sea ice. The frequent occurrence of negative nss-SO₄ values in the ice core (Figure 2 and Table 1) indicates that the transport of sea salts from the surface of newly formed sea ice is likely to represent an important process in the transfer of sea salt from the ocean to the ice core site, particularly around the time of the winter sea ice maximum [Wolff *et al.*, 2003]. However, for this coastal ice core it is the amount of open water within the marginal sea ice zone that appears to represent the main source of interannual variability in the sea salt signal of sea ice conditions. On an

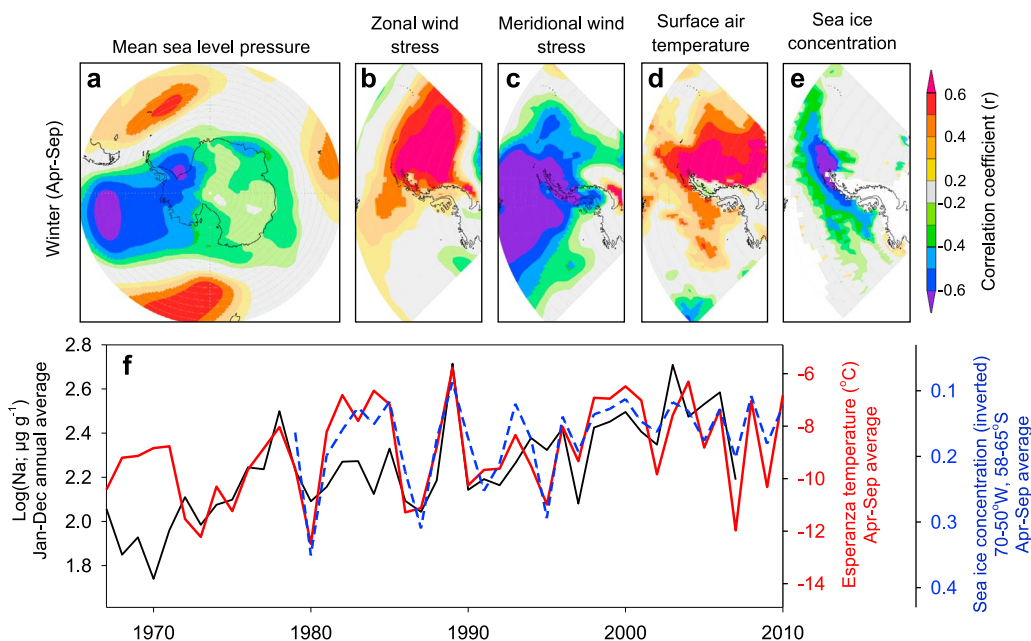


Figure 8. Spatial correlations of annual (Jan–Dec) averages of $\log(\text{Na})$ in the James Ross Island core with winter (Apr–Sep) averages of (a) mean sea level pressure, (b) zonal wind stress, (c) meridional wind stress and (d) surface air temperature in the ERA-Interim reanalysis (1989–2008), and (e) with sea ice concentration (1979–2008). Correlations that fall below 90% confidence are masked. (f) Time series of annual (Jan–Dec) average $\log(\text{Na})$ with winter (Apr–Sep) averages of temperatures at Esperanza (red solid) and sea ice concentration (blue dashed) in the 70–50°W, 58–65°S region where significant correlations exist (Figure 8e).

interannual timescale, sea ice concentration and northwesterly wind strength in this region covary, with northwesterly winds being associated with warmer conditions and less sea ice around James Ross Island (Figure 8d). This covariance means that the combined source and transport effects on sea salt variability act together to strengthen the environmental signal preserved in the sea salt concentration of the James Ross Island ice core.

[32] Building on this, the sea salt record from the James Ross Island ice core is found to correlate significantly with winter temperature at Esperanza station ($r = 0.58$, $p = 0.0001$, $n = 40$; Figure 8f). This association between increased annual average sea salt and warmer winter temperatures is seen in both the interannual variability and the long-term trends of the sea salt data, and is of equivalent strength to the relationship of winter isotope values in the James Ross Island core with winter temperatures (Table 2). In paleoclimate reconstructions from ice cores it is usually not possible to differentiate annual average isotope changes into their summer and winter components as the seasonal signal becomes muted by diffusion and thinning of annual ice layers [Cuffey and Steig, 1998]. The strong correspondence of annual average sea salt with winter temperatures in the region around James Ross Island means that the combined use of isotopic and sea salt signals in this core has the potential to overcome this limitation and allow for an evaluation, at least in a qualitative sense, of how past changes in temperature in this region relate to changes in the summer and winter season.

3.4. Marine Biogenic Compounds

[33] Methanesulphonic acid (MSA) in Antarctic ice cores is derived from the oxidation of dimethylsulphide that is released by marine algae [Mulvaney *et al.*, 1992; Ravishankara *et al.*, 1997; Legrand and Pasteur, 1998]. The oxidation of dimethylsulphide is also the major contributor to the non sea salt fraction of sulphate in Antarctic ice, although nss-SO_4 also has additional minor sources from volcanic emissions and pollution [Wolff *et al.*, 2006]. The marine algae that emit dimethylsulphide are particularly productive in the marginal sea ice zone around Antarctica [Curran and Jones, 2000] and this has led to numerous studies exploring the use of MSA as a proxy for sea ice extent around Antarctica [Curran *et al.*, 2003; Abram *et al.*, 2007; Abram *et al.*, 2010]. At ice core sites along the western and northern Antarctic Peninsula, including a previous ice core from James Ross Island, increased MSA has been shown to be significantly correlated with increased winter sea ice extent in the Bellingshausen Sea which is believed to enhance biological productivity during sea ice melting in the following spring/summer [Abram *et al.*, 2010]. A similar study in the Weddell Sea, however, showed that this relationship between increased MSA and more extensive sea ice in the previous winter does not exist at all locations around Antarctica [Abram *et al.*, 2007]. It was hypothesized that this may be due to the additional influence of transport distance, and that for some ice core sites wind speed and direction could play a more dominant role than source region production in determining the amount of MSA deposited in the ice.

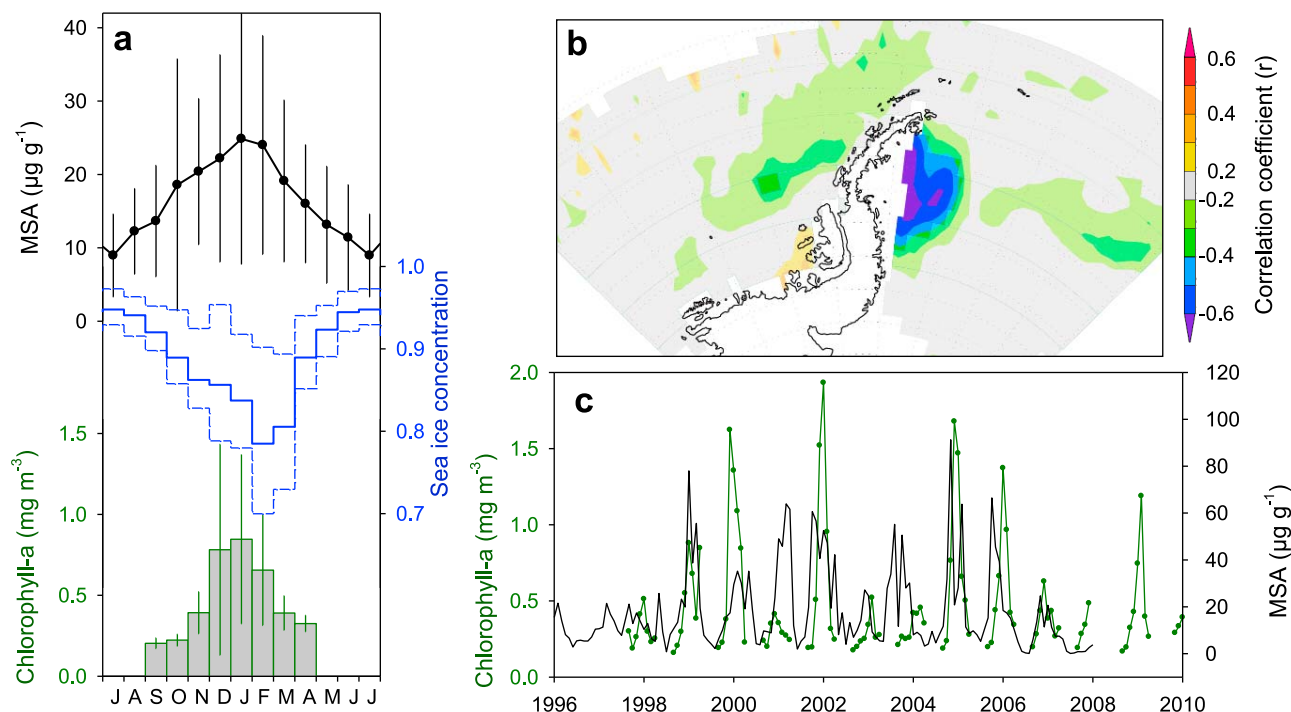


Figure 9. (a) The average annual cycle of MSA (black circles) in the James Ross Island core shown alongside the annual cycle of sea ice concentration in the 60–50°W, 64–72°S region (blue solid line) and chlorophyll-a concentrations in the 60–50°W, 62–68°S region (green bars; note the more northerly region and no data between May–August due to difficulties in detecting chlorophyll-a at high latitudes in the winter months). Error bars/dashed vertical line plots give the 1σ range on the composite monthly means. (b) Spatial correlation of annual (Jul–Jun) average MSA with summer (Oct–Mar) sea ice concentration (1979–2008). Correlations that fall below 90% confidence are masked. (c) Time series of monthly MSA (black) in the James Ross Island core with SeaWiFS chlorophyll-a concentration (green) in the region spanning 60–50°W, 62–68°S.

[34] The mean annual cycle of MSA and nss- SO_4 in the James Ross Island ice core shows a summer maximum that extends from November to April (Figure 9a). This is in agreement with studies from other sites around Antarctica [Mulvaney *et al.*, 1992; Legrand and Pasteur, 1998; Pasteur and Mulvaney, 1999] where the deposition of marine biogenic species show a summer peak and winter minimum. Correlation results are presented below using MSA as the representative marine biogenic species, however all of the results are reproducible by instead using nss- SO_4 .

[35] A record of MSA from an earlier ice core from James Ross Island has been shown to have a positive correlation with winter sea ice extent in the Bellingshausen Sea which is in agreement with MSA records from other sites along the western Antarctic Peninsula [Abram *et al.*, 2010]. This previous record extended to 1990 and repeating the analysis using the portion of our new, higher resolution MSA record for the portion of the ice core before 1990 confirms the previous result. However, when the analysis is carried out over the whole length of the new record that provides a much longer overlap with satellite sea ice records, this positive correlation with winter sea ice extent in the Bellingshausen Sea is found to be no longer significant. Instead, the James Ross Island MSA record shows a significant negative correlation with sea ice concentration in the region extending southward from James Ross Island along the eastern margin of the Antarctic Peninsula (Figure 9b). The

negative correlation of mean annual MSA with sea ice in this region is most significant over the summer half of the year spanning the time of sea ice melting through to the summer sea ice minimum. Using mean summer (Oct–Mar) sea ice concentration over the region spanning 60–50°W, 64–72°S, the correlation coefficient with mean annual ice core MSA is -0.61 ($p = 0.0004$, $n = 29$). The negative association between MSA and summer sea ice in this region of the Weddell Sea appears to be dominated by a strong association of low sea ice/high MSA years particularly from 1992 onwards (Figure 10).

[36] The new James Ross Island ice core also allows for a comparison of the marine biogenic compounds with satellite observations of SeaWiFS chlorophyll-a concentration which are available since September 1997. There is a good correspondence between both the timing and magnitude of MSA concentration in the James Ross Island ice core with chlorophyll-a concentration in the region spanning 60–50°W, 62–68°S (Figure 9). Note that a slightly different geographical region is used for chlorophyll-a compared with the region of maximum correlation with sea ice due to limitations in the SeaWiFS instrument detecting chlorophyll levels at high latitudes from autumn through to spring. The short length of the SeaWiFS record precludes a reliable calculation of statistical significance, however on interannual time scales the correlation of mean annual MSA with summer (Oct–Mar)

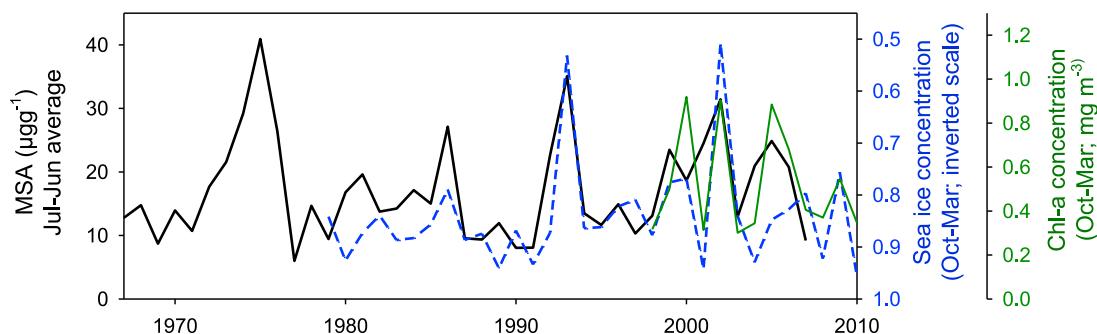


Figure 10. Annual (Jul–Jun) average MSA concentration (black solid) shown alongside summer (Oct–Mar) sea ice concentration in the region 60–50°W, 64–72°S (blue dashed; inverted scale) and chlorophyll-a concentration in the region 60–50°W, 62–68°S (green solid).

chlorophyll-a in the region to the south of James Ross Island has an r value of roughly 0.55 (Figure 10).

[37] Our results suggest that, at least over recent years, the marine biogenic compounds in ice from James Ross Island reflect a local summer-dominated source that is enhanced when summer sea ice is reduced (i.e., more open water is present), particularly in the area immediately offshore of the eastern Antarctic Peninsula in the Larsen ice shelf region. This is characteristic of the previous findings for marine biogenic species in the Dolleman Island ice core from the eastern side of the Antarctic Peninsula. Here, it was suggested that local sources from productivity within leads in the Weddell Sea ice pack were the primary contributor of marine biogenic species to the ice core [Pasteur *et al.*, 1995]. The increased influence of local biogenic sources at James Ross Island during recent decades could be related to the loss of ice shelves such as the Prince Gustav, Larsen A and Larsen B ice shelves near to James Ross Island [Pudsey and Evans, 2001; Pudsey *et al.*, 2006] which have allowed more local areas of summer open water to form. Satellite imagery shows that winter sea ice in this area of the western Weddell Sea now has a high contribution from first year ice (T. Maksym, personal communication, 2011) and during the summer has open water with high productivity [Hoppema *et al.*, 2000; Bertolin and Schloss, 2009]. Correlation of summer sea ice concentration in the 60–50°W, 64–72°S region with ERA-Interim reanalysis shows that years of reduced sea ice here are strongly correlated with strengthened northerly and westerly winds across the Weddell Sea. This is consistent with the climate anomalies that are associated with warming of the Antarctic Peninsula and Weddell Sea, and with analysis demonstrating a connection between the strength of the SAM and interannual sea ice variability in the Weddell Sea [Lefebvre *et al.*, 2004].

[38] For paleoclimate applications, the potential for changing sources of marine biogenic compounds at James Ross Island needs to be considered in the application of these proxies to reconstructing past sea ice changes. Prior to 1990, significant correlations with winter sea ice extent and the agreement of the James Ross Island MSA record with similar ice core records from the western Antarctic Peninsula [Abram *et al.*, 2010] provide strong evidence that when ice shelves have been present along the eastern Antarctic Peninsula the source of marine biogenic compounds at James Ross Island has primarily reflected a more distant Bellingshausen Sea source. The examination of changes in

marine biogenic compounds should thus be assessed alongside isotopic evidence for temperature changes, and other evidence for ice shelf history in the region [Pudsey and Evans, 2001; Pudsey *et al.*, 2006], to assess the likelihood of a significant contribution of local productivity sources in areas which until recently were permanently ice covered. This will be particularly important in interpreting the marine biogenic ice core record over the full Holocene record of the James Ross Island ice core.

4. Conclusions

[39] This detailed analysis of the environmental signals that are preserved in the most recent 40 years of the James Ross Island ice core provides a sound framework for using the rest of the ice core to reconstruct the paleoclimatic history of the northern Antarctic Peninsula region. Our key findings indicate that:

[40] 1. Comparison with the ice core accumulation and isotope record suggests that the higher resolution ERA-Interim reanalysis provides an improved representation over the older, lower resolution ERA-40 reanalysis of the meteorological conditions experienced at James Ross Island.

[41] 2. Accumulation variability at this site is influenced by the strength of the circumpolar westerly winds, with times of weaker winds allowing more precipitation events to reach the northeastern part of the Antarctic Peninsula. At the same time, this causes a decrease in accumulation along the western side of the Antarctic Peninsula which suggests that combining the accumulation record from James Ross Island with similar records from the western Antarctic Peninsula could strengthen the interpretation of how past changes in accumulation at James Ross Island relate to the strength of the circumpolar westerlies and the Southern Annular Mode.

[42] 3. The isotope signal in the James Ross Island ice core reflects changes in temperature at the site with a dependence of approximately 0.70 to 0.86 ‰ °C⁻¹ for $\delta^{18}\text{O}$, and 6.4 to 6.9 ‰ °C⁻¹ for δD . The annual average isotope signal preserves information about temperature variability in the summer and winter seasons. Interannual temperature variability in summer is associated with the strength of the Southern Annular Mode, while in the winter the temperature variability is related to pressure differences between the Amundsen Sea Low and high pressure in the southern Atlantic Ocean. Both of these climate features influence the strength of northerly wind anomalies across Drake Passage

and the Antarctic Peninsula and westerly wind anomalies across the northern Weddell Sea that result in warming at James Ross Island and the surrounding regions of the Weddell and Bellingshausen Seas.

[43] 4. The sea salt concentration in the ice core has a winter maximum and is derived from open water within the marginal sea ice zone to the north of James Ross Island and transported to the site by northwesterly winds. These sea ice and wind anomalies covary with temperature, giving the sea salt concentration in the James Ross Island core a significant correlation with winter temperatures that is of the same strength as the relationship between winter temperature and the isotopic concentration in the core. This suggests that the isotopic and sea salt signals could be used together to deconvolve the seasonal contribution to past temperature changes in the paleoclimate record from James Ross Island.

[44] 5. The source of marine biogenic compounds in recent decades has been summer productivity in open water areas within the Weddell sea ice pack to the south of James Ross Island. It appears that this represents a change in the dominant source region to more local productivity since the collapse of the ice shelves in the vicinity of James Ross Island. Prior to this, marine biogenic species at the James Ross Island site appeared to have a more distant source related to sea ice extent in the Bellingshausen Sea, consistent with similar records from the western Antarctic Peninsula. The potential for changes in the dominant source region indicates that past changes in the concentration of marine biogenic compounds at James Ross Island should be assessed alongside other evidence for paleoclimate changes.

[45] **Acknowledgments.** We thank Jack Triest, Sue Foord, Louise Sime, Olivier Alemany and Samantha Shelley, who helped to drill the James Ross Island ice core, and Emilie Capron, Louise Fleet and Emily Ludlow for laboratory assistance. We also gratefully acknowledge Geert Jan van Oldenberg and the KNMI Climate Explorer resource that aided the data analysis performed in this study (<http://climexp.knmi.nl>), and Gareth Marshall and the READER project for making the Antarctic station data available (www.antarctica.ac.uk/met/READER). Eric Wolff, Louise Sime, John King, Tom Bracegirdle and Ted Maksym provided helpful discussions during the preparation of this manuscript. This study is part of the British Antarctic Survey Polar Science for Planet Earth Programme. It was funded by the Natural Environment Research Council.

References

- Abram, N. J., R. Mulvaney, E. W. Wolff, and M. Mudelsee (2007), Ice core records as sea ice proxies: An evaluation from the Weddell Sea region of Antarctica, *J. Geophys. Res.*, **112**, D15101, doi:10.1029/2006JD008139.
- Abram, N. J., E. R. Thomas, J. R. McConnell, R. Mulvaney, T. J. Bracegirdle, L. C. Sime, and A. J. Arístarain (2010), Ice core evidence for a 20th century decline of sea ice in the Bellingshausen Sea, Antarctica, *J. Geophys. Res.*, **115**, D23101, doi:10.1029/2010JD014644.
- Acker, J. G., and G. Leptoukh (2007), Online analysis enhances use of NASA Earth science data, *Eos Trans. AGU*, **88**, 2, doi:10.1029/2007EO020003.
- Arístarain, A. J., and R. J. Delmas (2002), Snow chemistry measurements on James Ross Island (Antarctic Peninsula) showing sea-salt aerosol modifications, *Atmos. Environ.*, **36**, 765–772, doi:10.1016/S1352-2310(01)00362-4.
- Arístarain, A. J., R. J. Delmas, and M. Briat (1982), Snow chemistry on James Ross Island (Antarctic Peninsula), *J. Geophys. Res.*, **87**, 1005–1012, doi:10.1029/JC087iC13p11004.
- Arístarain, A. J., J. Jouzel, and C. Lorius (1990), A 400 years isotope record of the Antarctic Peninsula climate, *Geophys. Res. Lett.*, **17**, 2369–2372, doi:10.1029/GL017i013p02369.
- Arístarain, A. J., R. J. Delmas, and M. Stievenard (2004), Ice-core study of the link between sea-salt aerosol, sea-ice cover and climate in the Antarctic Peninsula area, *Clim. Change*, **67**, 63–86, doi:10.1007/s10584-004-0708-6.
- Berrisford, P., D. Dee, K. Fielding, M. Fuentes, P. W. Kallberg, S. Kobayashi, and S. M. Uppala (2009), The ERA-Interim archive, 16 pp., Eur. Cent. for Medium-Range Weather Forecasts, Reading, U. K.
- Bertolin, M. L., and I. R. Schloss (2009), Phytoplankton production after the collapse of the Larsen A ice shelf, Antarctica, *Polar Biol.*, **32**, 1435–1446, doi:10.1007/s00300-009-0638-x.
- Cavalieri, D. J., and C. L. Parkinson (2008), Antarctic sea ice variability and trends, 1979–2006, *J. Geophys. Res.*, **113**, C07004, doi:10.1029/2007JC004564.
- Cavalieri, D. J., C. Parkinson, P. Gloersen, and H. J. Zwally (2008), Sea ice concentrations from Nimbus-7 SMMR and DMSP SSM/I passive microwave data [digital media], http://nsidc.org/data/docs/daac/nsidc0051_gsfsc_seaice.gd.html, Natl. Snow and Ice Data Cent., Boulder, Colo.
- Cook, A. J., A. J. Fox, D. G. Vaughan, and J. G. Ferrigno (2005), Retreating glacier fronts on the Antarctic Peninsula over the past half-century, *Science*, **308**, 541–544, doi:10.1126/science.1104235.
- Cuffey, K. M., and E. J. Steig (1998), Isotopic diffusion in polar firn: Implications for interpretation of seasonal climate parameters in ice-core records, with emphasis on central Greenland, *J. Glaciol.*, **44**, 273–284.
- Curran, M. A. J., and G. B. Jones (2000), Dimethyl sulfide in the Southern Ocean: Seasonality and flux, *J. Geophys. Res.*, **105**, 20,451–20,459, doi:10.1029/2000JD900176.
- Curran, M. A. J., T. D. van Ommen, V. I. Morgan, K. L. Phillips, and A. S. Palmer (2003), Ice core evidence for Antarctic sea ice decline since the 1950s, *Science*, **302**, 1203–1206, doi:10.1126/science.1087888.
- Delmas, R. J., M. Legrand, A. J. Arístarain, and F. Zanolini (1985), Volcanic deposits in Antarctic snow and ice, *J. Geophys. Res.*, **90**, 2901–2920, doi:10.1029/JD090iD07p12901.
- EPICA community members (2004), Eight glacial cycles from an Antarctic ice core, *Nature*, **429**, 623–628.
- Fischer, H., et al. (2007), Reconstruction of millennial changes in dust emission, transport and regional sea ice coverage using the deep EPICA ice cores from the Atlantic and Indian Ocean sector of Antarctica, *Earth Planet. Sci. Lett.*, **260**, 340–354, doi:10.1016/j.epsl.2007.06.014.
- Hoppema, M., L. Goeyens, and E. Fährbach (2000), Intense nutrient removal in the remote area off Larsen Ice Shelf (Weddell Sea), *Polar Biol.*, **23**, 85–94, doi:10.1007/s0030000050012.
- Johnsen, S. J., H. B. Clausen, K. M. Cuffey, G. Hoffmann, J. Schwander, and T. Creyts (2000), Diffusion of stable isotopes in polar firn and ice: The isotope effect in firn diffusion, in *Physics of Ice Core Records*, edited by T. Hondoh, pp. 121–140, Hokkaido Univ. Press, Sapporo, Japan.
- Jouzel, J., F. Vimeux, N. Caillon, G. Delaygue, G. Hoffmann, V. Masson-Delmotte, and F. Parrenin (2003), Magnitude of isotope/temperature scaling for interpretation of central Antarctic ice cores, *J. Geophys. Res.*, **108**(D12), 4361, doi:10.1029/2002JD002677.
- Kreutz, K. J., P. A. Mayewski, I. I. Pittalwala, L. D. Meeker, M. S. Twickler, and S. I. Whitlow (2000), Sea level pressure variability in the Amundsen Sea region inferred from a West Antarctic glaciochemical record, *J. Geophys. Res.*, **105**, 4047–4059, doi:10.1029/1999JD901069.
- Lefebvre, W., H. Goosse, R. Timmermann, and T. Fichefet (2004), Influence of the Southern Annular Mode on the sea ice-ocean system, *J. Geophys. Res.*, **109**, C09005, doi:10.1029/2004JC002403.
- Legrand, M., and E. C. Pasteur (1998), Methane sulfonic acid to non-sea-salt sulfate ratio in coastal Antarctic aerosol and surface snow, *J. Geophys. Res.*, **103**, 10,991–11,006, doi:10.1029/98JD00929.
- Littot, G. C., R. Mulvaney, R. Rothlisberger, R. Udisti, E. W. Wolff, E. Castellano, M. De Angelis, M. E. Hansson, S. Sommer, and J. P. Steffensen (2002), Comparison of analytical methods used for measuring major ions in the EPICA Dome C (Antarctica) ice core, *Ann. Glaciol.*, **35**, 299–305, doi:10.3189/172756402781817022.
- Marshall, G. J. (2003), Trends in the southern annular mode from observations and reanalyses, *J. Clim.*, **16**, 4134–4143, doi:10.1175/1520-0442(2003)016<4134:TITSAM>2.0.CO;2.
- Masson-Delmotte, V., et al. (2008), A review of Antarctic surface snow isotopic composition: Observations, atmospheric circulation, and isotopic modeling, *J. Clim.*, **21**, 3359–3387, doi:10.1175/2007JCLI2139.1.
- McClain, C. R., G. C. Feldman, and S. B. Hooker (2004), An overview of the SeaWiFS project and strategies for producing a climate research quality global bio-optical time series, *Deep Sea Res., Part II*, **51**, 5–42, doi:10.1016/j.dsr2.2003.11.001.
- McConnell, J. R., A. J. Arístarain, J. R. Banta, P. R. Edwards, and J. C. Simoes (2007), 20th-century doubling in dust archived in an Antarctic Peninsula ice core parallels climate change and desertification in South America, *Proc. Natl. Acad. Sci. U. S. A.*, **104**, 5743–5748, doi:10.1073/pnas.0607657104.
- Miles, G. M., G. J. Marshall, J. R. McConnell, and A. J. Arístarain (2008), Recent accumulation variability and change on the Antarctic Peninsula

- from the ERA40 reanalysis, *Int. J. Climatol.*, 28, 1409–1422, doi:10.1002/joc.1642.
- Mulvaney, R., E. C. Pasteur, D. A. Peel, E. S. Saltzman, and P.-Y. Whung (1992), The ratio of MSA to non-sea-salt sulphate in Antarctic Peninsula ice cores, *Tellus, Ser. B*, 44, 295–303.
- Pasteur, E. C., and R. Mulvaney (1999), Laboratory study of the migration of methane sulphonate in firn, *J. Glaciol.*, 45, 214–218, doi:10.3189/002214399793377202.
- Pasteur, E. C., R. Mulvaney, D. A. Peel, E. S. Saltzman, and P.-Y. Whung (1995), A 340 year record of biogenic sulphur from the Weddell Sea area, Antarctica, *Ann. Glaciol.*, 21, 169–174.
- Petit, J. R., et al. (1999), Climate and atmospheric history of the past 420,000 years from the Vostok ice core, Antarctica, *Nature*, 399, 429–436, doi:10.1038/20859.
- Pudsey, C. J., and J. Evans (2001), First survey of Antarctic sub-ice shelf sediments reveals mid-Holocene ice shelf retreat, *Geology*, 29, 787–790, doi:10.1130/0091-7613(2001)029<0787:FSOASI>2.0.CO;2.
- Pudsey, C. J., J. W. Murray, P. Appleby, and J. Evans (2006), Ice shelf history from petrographic and foraminiferal evidence, northeast Antarctic Peninsula, *Quat. Sci. Rev.*, 25, 2357–2379, doi:10.1016/j.quascirev.2006.01.029.
- Rankin, A. M., E. W. Wolff, and R. Mulvaney (2004), A reinterpretation of sea-salt records in Greenland and Antarctic ice cores?, *Ann. Glaciol.*, 39, 276–282, doi:10.3189/172756404781814681.
- Ravishankara, R. A., Y. Rudich, R. Talukdar, and S. B. Barone (1997), Oxidation of atmospheric reduced sulphur compounds: Perspective from laboratory studies, *Philos. Trans. R. Soc. London B*, 352, 171–182, doi:10.1098/rstb.1997.0012.
- Rothlisberger, R., X. Crosta, N. J. Abram, L. Armand, and E. W. Wolff (2010), Potential and limitations of marine and ice core sea ice proxies: An example from the Indian Ocean sector, *Quat. Sci. Rev.*, 29, 296–302, doi:10.1016/j.quascirev.2009.10.005.
- Sime, L. C., J. C. Tindall, E. W. Wolff, W. M. Connolley, and P. J. Valdes (2008), Antarctic isotopic thermometer during a CO₂ forced warming event, *J. Geophys. Res.*, 113, D24119, doi:10.1029/2008JD010395.
- Sime, L. C., G. J. Marshall, R. Mulvaney, and E. R. Thomas (2009), Interpreting temperature information from ice cores along the Antarctic Peninsula: ERA40 analysis, *Geophys. Res. Lett.*, 36, L18801, doi:10.1029/2009GL038982.
- Smith, R. J. (2009), Use and misuse of the reduced major axis for line-fitting, *Am. J. Phys. Anthropol.*, 140, 476–486, doi:10.1002/ajpa.21090.
- Solow, A. R., and A. Huppert (2004), A potential bias in coral reconstructions of sea surface temperature, *Geophys. Res. Lett.*, 31, L06308, doi:10.1029/2003GL019349.
- Stenni, B., et al. (2010), The deuterium excess records of EPICA Dome C and Dronning Maud Land ice cores (East Antarctica), *Quat. Sci. Rev.*, 29, 146–159, doi:10.1016/j.quascirev.2009.10.009.
- Thomas, E. R., and T. J. Bracegirdle (2009), Improving ice core interpretation using in situ and reanalysis data, *J. Geophys. Res.*, 114, D20116, doi:10.1029/2009JD012263.
- Thomas, E. R., G. J. Marshall, and J. R. McConnell (2008), A doubling in snow accumulation in the western Antarctic Peninsula since 1850, *Geophys. Res. Lett.*, 35, L01706, doi:10.1029/2007GL032529.
- Thomas, E. R., P. F. Dennis, T. J. Bracegirdle, and C. Franzke (2009), Ice core evidence for significant 100-year regional warming on the Antarctic Peninsula, *Geophys. Res. Lett.*, 36, L20704, doi:10.1029/2009GL040104.
- Thompson, L. G., D. A. Peel, E. Mosley-Thompson, R. Mulvaney, J. Dai, P. N. Lin, M. E. Davis, and C. F. Raymond (1994), Climate since AD1510 on Dyer Plateau, Antarctic Peninsula: Evidence for recent climate change, *Ann. Glaciol.*, 20, 420–426, doi:10.3189/172756494794587438.
- Turner, J., S. R. Colwell, G. J. Marshall, T. A. Lachlan-Cope, A. M. Carleton, P. D. Jones, V. Lagun, P. A. Reid, and S. Iagovkina (2005), Antarctic climate change during the last 50 years, *Int. J. Climatol.*, 25, 279–294, doi:10.1002/joc.1130.
- Uppala, S. M., et al. (2005), The ERA-40 re-analysis, *Q. J. R. Meteorol. Soc.*, 131, 2961–3012, doi:10.1256/qj.04.176.
- van Ommen, T. D., and V. Morgan (2010), Snowfall increase in coastal East Antarctica linked with southwest Western Australian drought, *Nat. Geosci.*, 3, 267–272, doi:10.1038/ngeo761.
- Vaughan, D. G., G. J. Marshall, W. M. Connolley, C. Parkinson, R. Mulvaney, D. A. Hodgson, J. C. King, C. J. Pudsey, and J. Turner (2003), Recent rapid regional climate warming on the Antarctic Peninsula, *Clim. Change*, 60, 243–274, doi:10.1023/A:1026021217991.
- Wolff, E., A. M. Rankin, and R. Rothlisberger (2003), An ice core indicator of Antarctic sea ice production?, *Geophys. Res. Lett.*, 30(22), 2158, doi:10.1029/2003GL018454.
- Wolff, E. W., et al. (2006), Southern Ocean sea-ice extent, productivity and iron flux over the past eight glacial cycles, *Nature*, 440, 491–496, doi:10.1038/nature04614.

N. J. Abram, Research School of Earth Sciences, Australian National University, Canberra, ACT 0200, Australia. (nerilie.abram@anu.edu.au)
C. Arrowsmith, NERC Isotope Geosciences Laboratory, Keyworth NG12 5GG, UK.

R. Mulvaney, British Antarctic Survey, Cambridge CB3 0ET, UK.